Structures of vortex in Co-doped $BaFe_2As_2$ iron superconductors with different doping level by scanning Hall probe microscopy

Hussein Ali Mohammed
Department of Physics , Education Faculty for pure Secience , University of Kirkuk , Kirkuk , Iraq
hussein_ali722002@yahoo.com

Abstract
The 122 iron arsenide unconventional superconductors are part of a new class of iron-based superconductors. Co-doped $BaFe_{2x}Co_xAs_2$ (Ba-122) iron superconductors sample have been examine by scanning Hall probe microscopy (SHPM) technique to find out the magnetic properties of Ba-122 . Has been completed the evolution of profiles of vortices which has well isolated and it is as function of temperature, then utilized suitable technique to extract the temperature depending on penetration depth,$\lambda(T)$.So, this allowed to deduce the temperature dependent on density of superfluid and it has been compared with α-model consequences for a (2-band) of superconductor. When the superfluid density for the $BaFe_{2x}CoxAs_2$ (Over D x= 0.113) sample. As result, the two gap α-model has been fitted to the data with Δ_1=4.25kT_c, Δ_2=1.92kT_c , p=0.708, a_1=0.293 then a_2=1. However, When values of $\lambda(T)$ for the $BaFe_{2-x}Co_xAs_2$ (Over D x= 0.075) sample. Result of the superfluid density for $BaFe_{2-x}Co_xAs_2$ with parameters are (Δ_1=3.9k, Δ_2=1.6k), p=0.615 for Δ_1, and a_1=0.237, a_2=1. Suitable parameters produce refer into the symmetry of the order parameter at hole pockets with the electron, and then the relative supports of the bands to the density of superfluid in the iron-based crystals.

Keywords: GaAs/AlGaAs heterostructures, 2DEG Hall-probe sensor,scanning Hall probe microscopy technique.

Introduction
Early in 2006 superconductivity was found in LaFePO with a transition temperature T_c=5 K by Hosono's group. Around the same time, various families of transition-metal oxide were discovered to be superconducting with similar low transition temperatures. However, in January 2008 the superconductivity community was surprised by another breakthrough of Hosono's group when they reported that T_c=26 K in the closely related system $LaFeAsO_{1-x}F_x$ [1]. The highest value achieved by replacing La by Sm in $SmFeAsO_{0.9}F_{0.1}$ which was T_c=55K. The number of iron-based superconductors quickly increased after this as well as it is now divided into several families, for instance, the ternary '122' compounds MFe_2As_2 with the $ThCr_2Si_2$ crystal structure (M = Sr, Ba, Ca), so it is based on FeAs layers [2]. The compounds MFe_2As_2 have the simplest crystal structure, also the structural and magnetic transitions occur simultaneously in this material ($T_{n(s)}$=135K in $BaFe_2As_2$). Superconductivity has been discovered in different 122-compounds with hole or electron doping [3]. Furthermore, hydrostatic pressure can induce a superconducting state in the 122 - parent compounds for example $CaFe_2As_2$ $SrFe_2As_2$, and $BaFe_2As_2$.

Both the magnetic penetration depth, ($\lambda(T)$), temperature dependence are sensitive probes of the superconducting gap and order parameter. The advantage of these measurements are directly probe the normalised superfluid density, ($\overline{\rho_s} = (\lambda(0)^2/\lambda(T)^2)$). As result, to find out electrons numbers in (superconducting case). Scanning Hall probe microscopy (SHPM) technique was used in this work to find out temperature which is depending on$\lambda(T)$, by imaging single vortices of $BaFe_{2-x}Co_xAs_2$ samples in very high quality single crystals with different doping levels. A measure gap fitting technique which was used to find out the density of superfluid model, yielding understandings at the Fermi surface by both the number with structure of superconducting gaps [4].

Lately, but, which has have been shown very highly disordered vortices lattice in signal crystal sensor. So, reason behind that which is the introduction these defects by heavy ion irradiation be able to considerably improve,j_c, as well powerfully control the rates of sprawl vortex. Therefore, in order to understanding both vortex matter as well pinning potentials of these materials which that display significant to enable high current applications at the future [5, 6].

Experimental
GaAs/AlGaAs heterostructure sample is cleaved into (6 X 6) mm square chips. The chips are cleaned by three solvent cleaning steps in a standard way, namely keeping for 5 minutes in trichloroethylene, acetone and isopropanol, respectively in an ultrasonic bath at 18 % power. The chips are dried by high pressure nitrogen gas and then clean chips are stuck on glass cover slips using Shipley Micro posit S1813 photoresist with the active side facing up. Later, they are baked at 90^0 C for 30 minutes. Shipley Micro posit photoresist is spun onto the chips at 3500 rpm for 30 seconds to get a thick resist layer and baked in an oven at 90^0C for 10 minutes. So, the chips are soaked in chlorobenzene. To obtain the formation of an overhang profile when patterned. Again, the resist is baked for same time. To pattern Ohmic contacts, the resist is exposed for about 10 to 20 seconds using a Karl Suss (MJB3) mask aligner. These samples are then developed using Micro posit 351 developer.

The surface oxide of chips are removed by dipping them in a 1:1 HCl: H_2O solution for 20-30 seconds and the oxide is removed when these chips are

mounted in a thermal evaporator. The contact material such as 66nm of Ge, 134nm of Au, 10-20nm of Ti and 200nm of Au, are evaporated sequentially in the same operation under high vacuum ($3x10^{-6}$ mbar). As a result, the chips are annealed under forming gas (90 % N_2 and 10% H_2) at 415^0C for 10 seconds which it leads form good electrical contact to the 2DEG. The 2DEG regions between Ohmic contact leads are removed by wet chemical etching using same process as well as the resist was then stripped in acetone with the chips checked by an optical microscope. By the same way, all patterning and cleaning steps were performed for the Ohmic contacts except the resist spin speed was increased from (4000- 5000) rpm for 30 seconds. The sample tip was formed from a 10 nm of Ti thick layer and then followed by 50 nm layer of Au, without any annealing. The design for making the STM tip places it at the highest point near the corner of the Hall probe of sensors to ensure that it comes into contact with the sample first. Deep etching to a depth of ~1µm was performed in the same way as for coarse lead etching except the etching solution was (1:8:80) H_2SO_4:H_2O_2:H_2O with an approximate etch rate of 540 nm/min, shown in figure 1. After etching, the chips were cleaved into four Hall probes. The resist was then removed by the same way with acetone and isopropanol. The Hall sensors were mounted on a chip carrier using Oxford Instruments low temperature epoxy. The Ohmic contact leads were then bonded to the chip carrier using 25 µm diameter gold wire in an ultrasonic wire bonder. The chip carrier was then screwed onto the SHPM Head. The sample puck was then mounted on the SHPM Head then the angle between the sample plane and the Hall probe adjusted around1-2 degrees. Later, the system has cooled below T_c, a coarse 'stick-slip' approach mechanism was used for both the sample and Hall probe until a tunnel current was detected at the tip. The puck was then retracted one step, the corners of the sample checked and the sample scanned.

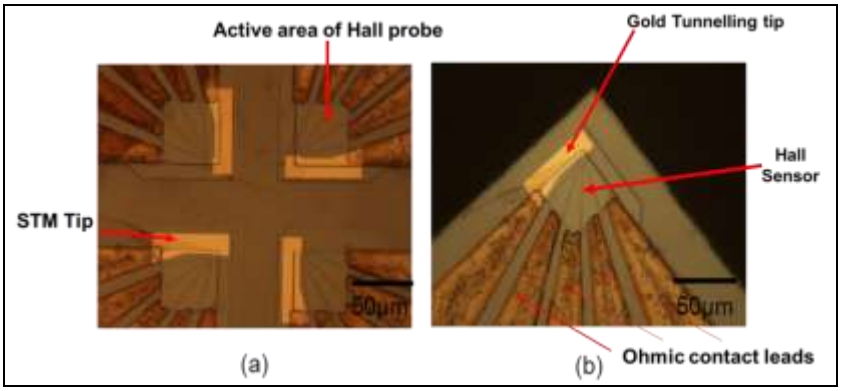

Figure 1. It shows optical images of the chip after: (a) deep etching, (b) cleaving.

Results and discussion

Both figures (2 and 3) show typical magnetization loops for $Ba(Fe_{0.93}Co_{0.07})_2As_2$ and $Ba(Fe_{0.89}Co_{0.11})_2As_2$ single crystals at different temperatures below T_c. These results were taken of the sample (Hall sensor) about (300-500) nm from the (surface of the crystal) with using magnetic field about (H=±70) G. The best measure of the diamagnetic screening about at (H_z=+/-25G) which graph is shown in figures (2 and 3) which are shows as a function of temperature. The diamagnetic signal above the critical temperature of both samples is probably due to weak diamagnetism in the normal state. Figure 2 appears the estimated value of the critical temperature Tc=23.3±0.05K of the Ba $(Fe_{0.93}Co_{0.07})_2As_2$ single crystal, which has been inferred from the intercept of the linear extrapolation of ΔM with temperature. Comparable data yielding the critical temperature (T_c =9.62±0.05K) of Ba $(Fe_{0.89}Co_{0.11})_2As_2$ single crystal shown in figure 3.

ISSN: 1813 – 1662 (Print)
E-ISSN: 2415 – 1726 (On Line)

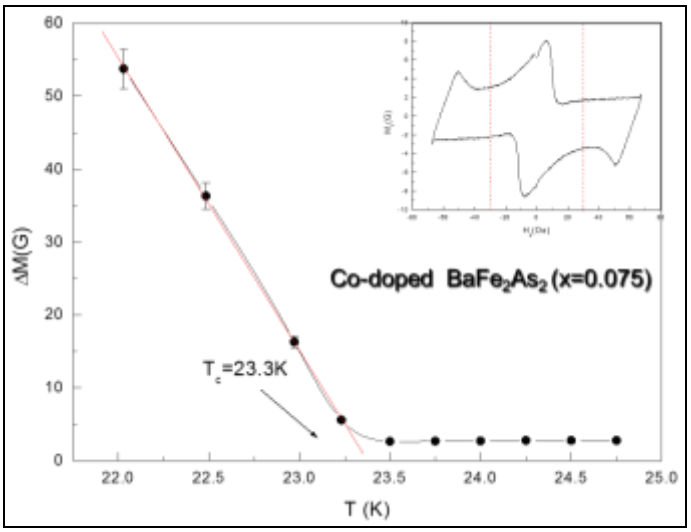

Figure 2. Dia-magnetic signal estimated of Ba $(Fe_{0.93}Co_{0.07})_2As_2$ single crystal. (The inset above displays a typical M_I–H_z captured at T =22.78 K)

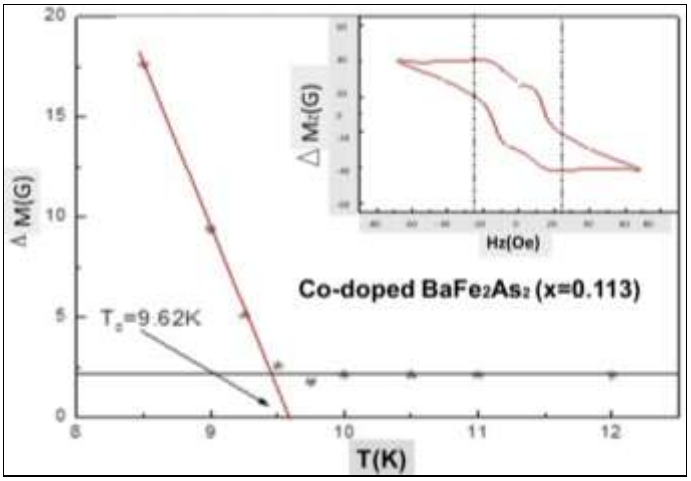

Figure 3. Dia-magnetic signal estimated of Ba $(Fe_{0.89}Co_{0.11})_2As_2$ single crystal. (The hysteresis loop taken at T =8.8K)

Several vortices images of sample (Ba $(Fe_{0.93}Co_{0.07})_2$) through temperature 12K resolved by (SHPM) technique (shows in Fig 4) with using magnetic fields(-6 to +2) G as well as somewhat of earth's field about -2G. The (Ba $(Fe_{0.93}Co_{0.07})_2$) sample has H_z=+1G from above T_c. Has noted that in this process, all images were crucial to capture by (SHPM) with every new temperature. These images are captured with size of scan about 9.0X9.0µm.

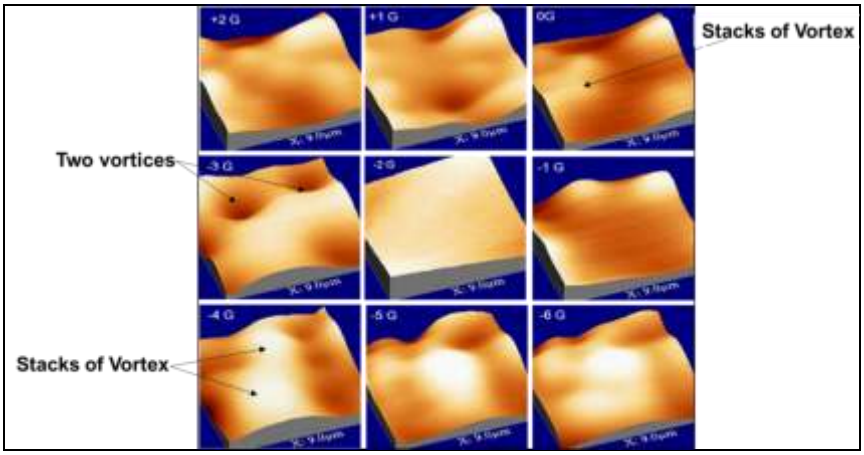

Figure 4. It shows images of vortices in a Ba $(Fe_{0.93}Co_{0.07})_2As_2$ single crystal images using scanning Hall probe microscopy technique

ISSN: 1813 – 1662 (Print)
E-ISSN: 2415 – 1726 (On Line)

In figure 5 illustration comparable vortices images captured by SHPM techinque starting at (6k from T>12K) on a (Ba $(Fe_{0.89}Co_{0.11})_2As_2$) single crystal in somewhat magnetic fields applied from(-5 to +5)G. Furthermore, earth's field around +2 G. These images are captured with size of scan about (7.0 X3.0) µm.

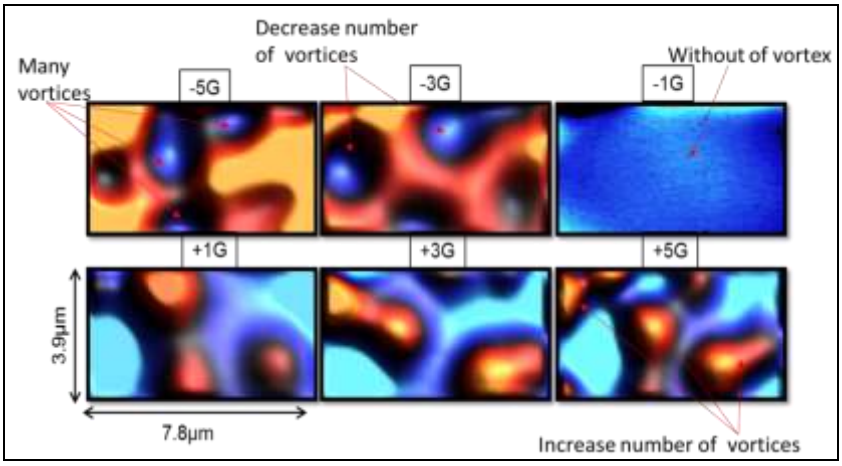

Figure 5. Images of the Co-doped Ba $(Fe_{0.89}Co_{0.11})_2As_2$ single crystal shows after field-cooling from above T_c = 12K slightly goes to T=6K in various applied magnetic fields from +5G to -5G.

It is well established that the temperature depending on density of the superfluid,$(\bar{\rho_s}(T))$, of $BaFe_{2x}Co_xAs_2$ single crystal samples which has been probed at various x-concentrations across the superconducting, optimally doped (OptD) x= 0.075 over doped (OD) x = 0.113. In addition, the magnetic penetration depth, $\lambda(T)$, dependent on temperature in $BaFe_{2x}Co_xAs_2$ (OptD x = 0.07), after field cooling at H=+1G at different temperatures up to T_c which it was extracted by fitting the magnetic profile of a well-isolated single vortex after field cooling at H=+1G at different temperatures up to T_c. A variation model due to Clem with a modification suggested by Kirtley et al [7,8] which it was used to fit the data assuming $\lambda(0)$=0.250 µm, and $\xi_v = 2.5\text{nm}/\sqrt{1-T/T_c}$, width (w), of Hall probe (an active part)about (800)nm with z = 2.295µm as a fit parameter. As previously mentioned, the temperature-dependent normalised superfluid density $(\rho_s(T)/\rho_s(0) = \lambda(0)^2/\lambda(T)^2)$ [9]. As a result, it was calculated using the extracted values of penetration depth. Basically, these data were then fitted to (2 band) α-model with (2 full gaps) and then it supposed to($\rho_s(T) = p\rho_1(T) + (1-p)\rho_2(T)$), where $(\rho_{1,2}(T))$ densities of superfluid in the dissimilar 2-bands with(ρ_s) are capture into measure the relative contribution from every one.

Densities of superfluid were calculated from equations (1), (2) as below: [10].

$$\rho_i(T) = 1 - \frac{1}{2kT}\int_0^\infty cosh^{-2}\left(\frac{\sqrt{\varepsilon^2+\Delta_i(T)^2}}{2kT}\right)d\varepsilon, \qquad (1)$$

Where the gap found via

$$\Delta_i(T) = \Delta_i(0)tanh\left[\frac{\pi kT_c}{\Delta_i(0)}\sqrt{a_i\left(\frac{T_c}{T}-1\right)}\right]. \qquad (2)$$

Here a_i refer to characteristic parameter which that meaning as following: (for instance, a_i=1, 4/3, 2 and 0.38 which firstly for isotropic s-wave pairing, secondly for two-dimensional d-wave, thirdly for s+g-wave and finally for nonmonotonic d-wave respectively) [11].

The best scan by SHPM technique is slightly superior than usually be expected as well as presumably the tilt angle of sensor is a bit better around 1^o (one degree) in this process. Nevertheless, in order to extraction values of $(\lambda(T))$, at dissimilar temperatures of $(\Delta\lambda(T) = \lambda(T) - \lambda(0))$ see figure 6. Where it shows the extracted values of $\lambda(T)$ for the $BaFe_{2-x}Co_xAs_2$ (OptD x = 0.075) sample and figure. The calculated superfluid density for $BaFe_{2-x}Co_xAs_2$ with parameters (Δ_1=3.9k, Δ_2=1.6k), p=0.615 for Δ_1, and a_1=0.237, a_2=1, [9,11].

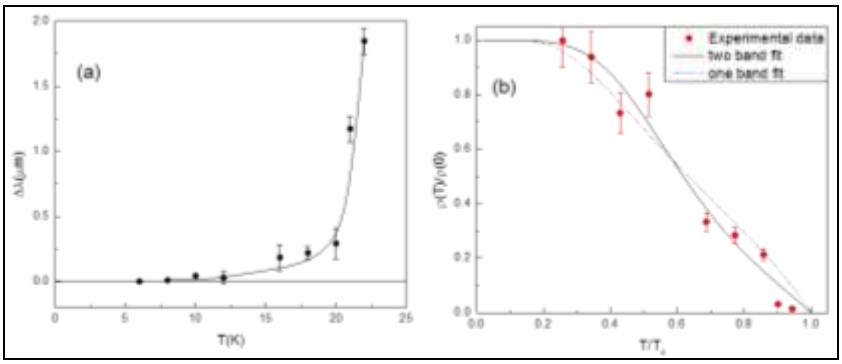

Figure 6. It shows (a) extracted from fits on the $BaFe_{2-x}Co_xAs_2$ (Opt. D x= 0.075) sample by $\Delta\lambda(T) = \lambda(T) - \lambda(0)$, which at (b) the red points appear the experimental the density of superfluid depending on the temperature (T).

At figure7 (a,b) displays comparable data for the temperature dependence on the superfluid density for the $BaFe_{2x}CoxAs_2$ (Over D x= 0.113) sample, which it was calculated by fitting $\Delta\lambda(T) = \lambda(T) - \lambda(0)$ on awell-isolated vortex at H=-1.5Oe where $\lambda(0)$=0.2752 μm , as well as z=1.547[9]. The two gap α-model has been fitted to the data with Δ_1=4.25kT_c, Δ_2=1.92kT_c , p=0.708, a_1=0.293 then a_2=1 [11,12].

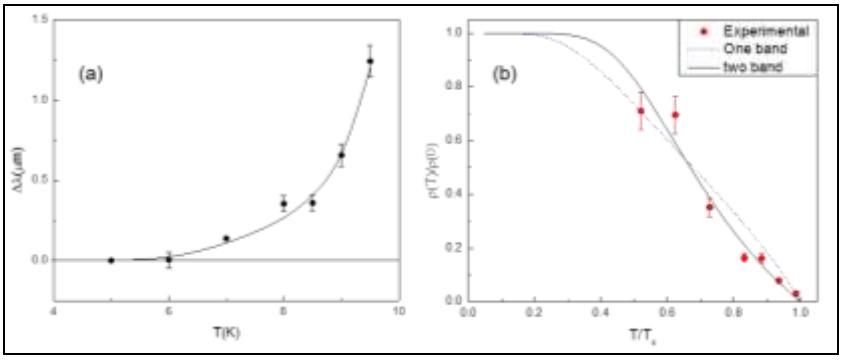

Figure 7. It shows (a) the $BaFe_{2x}Co_xAs_2$ (OverD x= 0.113) sample (b) red points show the experimental the density of superfluid depending on the temperature.

Both figures 6 and 7 show that the model of (2- gap) is a much best suitable to $\overline{\rho_s}(T)$ than model of (1-gap) and has an ≈8% lower root-mean-square (RMS) error, while the error bars are completely large. In addition, the fitted values of a_1=0.236 for $BaFe_{2-x}CoxAs_2$ (Opt. x= 0.075) then a_1=0.293 for $BaFe_{2-x}CoxAs_2$ (OverD x= 0.113) would tend to implicate non-monotonic d-wave symmetry for the superconductivity gap symmetry with 45° nodes characteristic of the d-wave order parameter [11]. But, these results disagree other results in electron-doped pnictides where it gives proof for s± wave pairing [12]. Nevertheless, several recent reports literatures propose that the pairing symmetry in the $BaFe_2As_2$ compound undergoes a transition from s to d symmetry with potassium doping up to the fully doped KFe_2As_2 compound which has been identified as a d-wave superconductor[13,14].

Conclusions

1- In order to find the temperature dependent on ($\lambda(T)$) in Co-doped $BaFe_2As_2$ single crystals has been used SHPM technique.

2- Our results have been modelled by assuming a picture of two fully gapped bands incorporating a free symmetry dependent parameter (a).

3- Analysis of vortex profiles has been made assuming that the small gap at the hole-like pockets is isotropic s-wave. Fit parameters suggest electron pockets have a strongly anisotropic OP in optimally doped Ba122 sample.

References

[1] Y. Kamihara, T. Watanabe, M. Hirano, and H. Hosono, Iron-Based Layered Superconductor La[O1-xFx]FeAs (x = 0.05−0.12) with Tc = 26 K. Journal of the American Chemical Society 130, (2008) 3296.

[2] P. Gao, Y. Zhang,Y. Zhang, and E. Hellstrom, Atomic and electronic structures of superconducting $BaFe_2As_2/SrTiO_3$ superlattices, PHYSICAL REVIEW B 91, (2015), 104525.

[3] P. L. Alireza, Y. T. Ko, , and S. E. Sebastian, Journal of physics. Condensed matter : an Institute of Physics journal 21, (2009), 012208.

[4] Y. Nakajima, Y. Tsuchiya, T. Taen, T. Tamegai, S. Okayasu, and M. Sasase, Enhancement of critical current density in Co-doped $BaFe_2As_2$ with columnar defects introduced by heavy-ion irradiation ,Physical Review B 80, (2009), 012510,

[5] M .N. Konzen and S. Sefat, Lattice Parameters Guide Superconductivity in Iron-Arsenides. Journal of Physics: Condensed Matter, 29 (2017), 083001.
[6] R. Prozorov, M. A. Tanatar, B. Shen, P. Cheng, H.-H. Wen, S. L. Bud'ko, and P. C. Canfield, Magnetic order in the purely organic quasi-one-dimensional ferromagnet 2-benzimidazolyl nitronyl nitroxide, Physical Review B 82, (2010),180513.
[7] K. Terashima, Y.Sekiba, J. H. and T. Takahashi, Fermi surface nesting induced strong pairing in iron-based superconductors. Proceedings of the National Academy of Sciences, 106(18), (2009). p. 7330-7333.
[8] R. H. Liu; G. Wu; and H. Chen;Transport properties and superconductivity in (M=La and K) with double FeAs layers. EPL (Europhysics Letters), 84(2), (2008), p. 27010.
[9] R.Prozorov and R.W.Giannetta, Superconductor Science and Technology 19, R41 (2006).
[10] A.C. Rose-Innes and A.C. Rhoderick, Introduction to Superconductivity,Pergamon Press, (1978).
[11] P. Gao, Y. Zhang, S. Y. Zhang, and Q. Pan, Atomic and electronic structures of superconducting $BaFe_2As_2/SrTiO_3$superlattices,PHYSICAL REVIEW, B 91, (2015), 104525.
[12] M. Reticcioli, G. Profeta, C. Franchini, A. Continenza, Ru-doping on iron based pnictides: the "unfolded" dominant role of structural effects for superconductivity. Journal of Physics: Condensed Matter,[v1],(2017),1701.
13] J. Bardeen and M. J. Stephen, Theory of the Motion of Vortices in Superconductors, Physical Review 140, (1965), A1197.
[14] P. W. Anderson and Y. B. Kim, Hard Superconductivity:Theory of the Motion of Abrikosov Flux Lines Reviews of Modern Physics 36, (1964), 39.

هياكل الدوامة في Co-doped $BaFe_2As_2$ الحديد الموصلات الفائقة مع مختلف مستويات التطعيم بواسطة المسح المجهر المايكروسكوبي.

حسين علي محمد

قسم الفيزياء ، كليةالتربية للعلوم الصرفة ، جامعة كركوك ، كركوك ، العراق

hussein_ali722002@yahoo.com

الملخص

تعتبر122 من الزرنيخ الحديد الموصلات الفائقة غير التقليدية هي جزء من فئة جديدة من الموصلات الفائقة القائمة على الحديد وتم فحص Co-doped BaFe2xCoxAs2 (Ba-122) عينات الموصلات الفائقة عن طريق استخدام تقنية مسح المجهر المايكروسكوبي لدراسة الخواص المغناطيسية. وتم الانتهاء من تطور شكل الدوامات التي لديها عزل بشكل جيد وأنها هي دالة لدرجة الحرارة، ثم استخدمت تقنية مناسبة لاستخراج درجة الحرارة اعتمادا على عمق الاختراق المغناطيسية. وهذا، بدوره، يتيح لنا أن نستنتج أن كثافة الموصلية الفائقة التي تعتمد على درجة الحرارة التي تم مقارنة النموذج مع نتائج النطاقين لمادة الموصل الفائق. عندما كثافة الطفو الفائق للنموذج (x= 0.113) BaFe2xCoxAs2 .

ونتيجة لهذا فان النموذج النطاقين تكون مناسبة مع القيم $\Delta1=4.25kTc$, $\Delta2=1.92kTc$, $p=0.708$, $a1=0.293$, $a2=1$ لكن عندما x= 0.075 لنفس النموذج فان المعلمات $a2=1$, $al=0.237$, $p=0.615$ for $\Delta1$, $\Delta2=1.6k$, $\Delta1=3.9k$ باستخدام معلمات مناسبة تنتج الأفكار الجيدة في نظام التماثل لتنظيم المعلمات عند الالكترون والفجوات فضلا عن المساهمات النسبية للنطاقات لكثافة الموصل الفائق.

الكلمات المفتاحية: مادة GaAs/AlGaAs وتقنية المسح المجهر المايكروسكوبي، مستشعر مجس هول.